Oxidative Cleavage of DNA by Ruthenium(II) Complexes Containing a Ferrocene/Non-Ferrocene Conjugated Imidazole Phenol Ligand

ARTICLE *in* ORGANOMETALLICS · SEPTEMBER 2012

Impact Factor: 4.13 · DOI: 10.1021/om3007882

4 AUTHORS, INCLUDING:

Sathyaraj Gopal
University of Madras
9 PUBLICATIONS **110** CITATIONS

SEE PROFILE

Balachandran Unni Nair
Central Leather Research Institute
370 PUBLICATIONS **6,244** CITATIONS

SEE PROFILE

ORGANOMETALLICS

Article

pubs.acs.org/Organometallics

Oxidative Cleavage of DNA by Ruthenium(II) Complexes Containing a Ferrocene/Non-Ferrocene Conjugated Imidazole Phenol Ligand

Gopal Sathyaraj,[†] Mathiyalagan Kiruthika,[†] Thomas Weyhermüller,[‡] and Balachandran Unni Nair*[,†]

[†]Chemical Laboratory, Central Leather Research Institute, CSIR, Adyar, Chennai 600020, India

[‡]Max-Planck Institut für Bioanorganische Chemie, D-45470 Mülheim an der Ruhr, Germany

Supporting Information

ABSTRACT: Three mixed-ligand ruthenium(II) complexes with general formula $[Ru(bpy)_2L](PF_6)$ (**1**−**3**), where L = 2-{4,5-bis[(*E*)-2-ferrocenylvinyl]-1*H*-imidazol-2-yl}phenol (**1**), 2-{4,5-bis[(*E*)-2-ferrocenylvinyl]-1*H*-imidazol-2-yl)-4,6-dichlorophenol (**2**), 2-{4,5-bis[(*E*)-2-(4-chlorophenyl)ethenyl]-1*H*-imidazol-2-yl}phenol (**3**), have been synthesized and characterized. All the three complexes bring about DNA cleavage in the presence of H_2O_2. Due to the presence of three redox-active metal centers in complexes **1** and **2** these two complexes show enhanced DNA cleaving activity in comparison to that exhibited by complex **3**, which contains only one redox-active metal center.

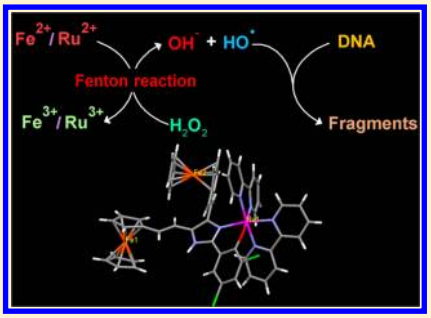

INTRODUCTION

During the past decade, the interest in the field of metal−nucleic acid interactions has burgeoned. The progress in this field is primarily because of the tremendous advances that have occurred in nucleic acid technology.[1] The modification of biological molecules with organometallic and classical coordination compounds has attracted much attention in recent years. A little more than 50 years have elapsed since the discovery of ferrocene, and during this period its chemistry has been developed quite extensively.[2] The stability of the ferrocenyl group in aqueous, aerobic media, the accessibility of a large variety of its derivatives, and its favorable electrochemical properties have made ferrocene and its derivatives very popular molecules for biological applications and for conjugation with biomolecules. Ferrocene itself exhibits interesting properties as an antianemic or cytotoxic agent. Conjugates of ferrocene with well-known antibiotics such as penicillins and cephalosporins have been reported.[3] In addition, structural variations of established drugs with the ferrocenyl moiety, such as ferrocenyl aspirin, the antimalarial drugs chloroquine (termed ferroquine), quinine, mefloquine, and artemisinin, and the anticancer drug tamoxifen (ferrocifen) have also been reported.[4] In addition to ferrocene-based compounds, arene−ruthenium complexes have been shown to be useful as antimetastasis agents to control tumor malignancy.[5]

DNA interaction studies on polypyridyl metal complexes have been the focus of several bioinorganic research groups. Polypyridyl complexes of ruthenium and rhodium exhibit interesting spectroscopic and luminescence properties on binding to DNA.[6] Ruthenium(II) polypyridyl complexes, because of their excellent redox and photophysical properties, low toxicity, and increased effectiveness toward primary tumors have the potential to serve as anticancer agents.[7] On the other hand, imidazole is a part of many important biological molecules and so has become a vital component of a large number of pharmacologically active molecules. The imidazole ring is coordinated to the transition-metal ions in a number of biologically important systems. These facts make imidazole and its derivatives important target analytes. It has been reported that the metal coordination compounds of imidazole could inhibit tumor growth by interacting with DNA.[8] Imidazole is present in the anticancer medicine mercaptopurine, which combats leukemia by interfering with DNA synthesis.[9] Phenolate ion, a hard base formed by hydrogen dissociation from phenolic molecules, stabilizes the higher oxidation states of ruthenium upon its coordination.

Taking into consideration the medicinal value associated with both ruthenium-based drugs and iron-based drugs, it is valuable to study their combined effects. A ferrocenyl unit conjugated to a complexed ruthenium(II) center may enhance the compound's ability to induce DNA damage. Furthermore, complexes having two redox-active metal centers may be able to provide multiple DNA-damaging pathways in photodynamic therapy. This would increase the chances of achieving successful DNA damage and, perhaps more significantly, increase the likelihood of providing a mechanism that is independent of oxygen. Therefore, by considering all the above, in the present investigation, we have isolated redox-active heteroleptic Ru(II) complexes of the general formula $[Ru(bpy)_2L](PF_6)$ (**1**−**3**), where L = 2-{4,5-bis[(*E*)-2-ferrocenylvinyl]-1*H*-imidazol-2-yl}phenol (**1**), 2-{4,5-bis[(*E*)-2-ferrocenylvinyl]-1*H*-imidazol-2-yl)-4,6-dichlorophenol (**2**), 2-{4,5-bis[(*E*)-2-(4-chlorophenyl)ethenyl]-1*H*-imidazol-2-yl}phenol (**3**), and have analyzed their DNA binding and cleaving properties.

Received: August 15, 2012
Published: September 20, 2012

dx.doi.org/10.1021/om3007882 | *Organometallics* 2012, 31, 6980−6987

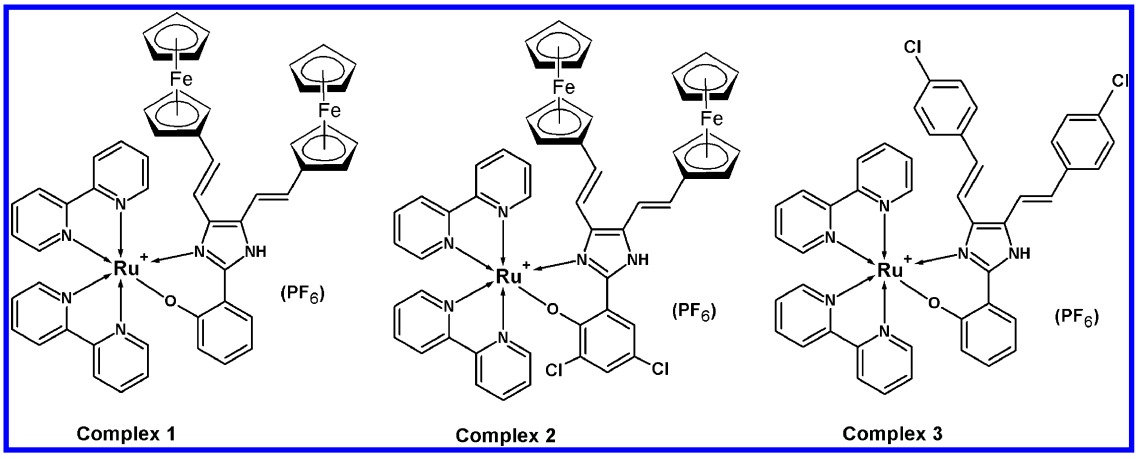

Figure 1. Structures of complexes **1**–**3**.

RESULTS AND DISCUSSION

Synthesis and Characterization of Mixed-Ligand Ru(II) Complexes. Mixed ligand Ru(II) complexes **1**–**3** (Figure 1) have been isolated as their hexafluorophosphate salts, purified by neutral alumina column chromatography with toluene/acetonitrile as eluent, and characterized by various techniques such as ESI-MS, FT-IR, UV–visible, elemental analysis, and cyclic and differential pulse voltammetry. All three complexes are discrete monomeric cationic molecules in solution, as evident from the mass spectral data. The ESI mass spectra of complexes **1**–**3** show base peaks corresponding to monomeric cationic species $(M - PF_6)^+$ at 993.00, 1061.93, and 845.07, respectively (Figure S1, Supporting Information). The compounds isolated here are racemic mixtures. Attempts to isolate enantiomerically pure compounds were unsuccessful. Electronic absorption spectra of all the three racemic complexes were recorded in acetonitrile solvent (Figure 2). The absorption peak maxima and the corresponding molar extinction coefficient values for various transitions in the complexes are shown in Table 1. It can be noted that all three complexes exhibit MLCT bands in the region of 520 nm as a broad, not well resolved peak arising from the ruthenium(II) complex. The d–d band of the ferrocene moiety of complexes **1** and **2** are observed as shoulder peaks at around 466 and 460 nm, close to the MLCT transition of the ruthenium(II) center. The ligand-centered $\pi-\pi^*$ transition is the most intense peak, which is observed around 292 nm for all three compounds. Ferrocene derivatives are known to be efficient fluorescence quenchers because of the photoinduced electron-transfer process.[10] Complexes **1** and **2** do not show any fluorescence upon excitation at their respective MLCT bands. Complex **3**, however, which lacks a ferrocenyl moiety, shows emission at 562 nm upon excitation at its MLCT band. Lack of emission for complexes **1** and **2** from their MLCT excited states is a clear indication that the presence of a ferrocenyl unit in the molecule quenches the excited state of the ruthenium(II) complex. The fluorescence spectra of the three complexes are shown in Figure 3.

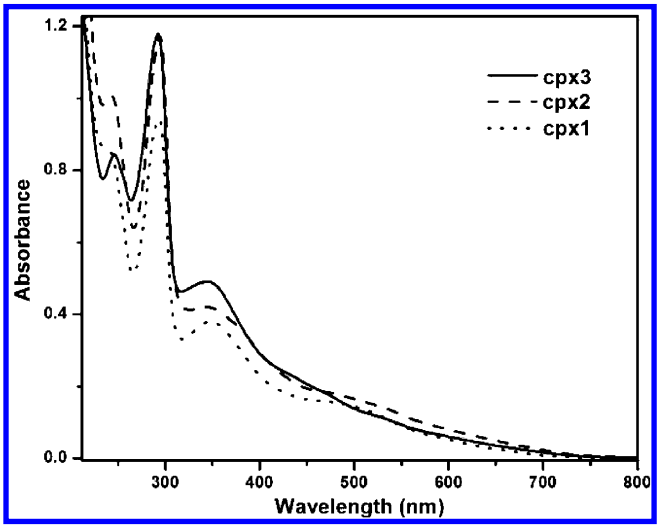

Figure 2. UV–visible spectra of complexes **1**–**3** in acetonitrile (20 μM).

The electrochemical properties of the three complexes were investigated in acetonitrile solution by employing cyclic (CV) and differential pulse voltammetry (DPV). The cyclic and differential pulse voltammogram of the complexes are depicted in parts a and b, respectively, of Figure 4, and the redox potentials are summarized in Table 1. The DPV of complex **1** shows two redox peaks at +0.353 and +0.485 V, which could be attributed to the Ru(II)/Ru(III) and Fe(II)/Fe(III) redox couples. The Ru(II)/Ru(III) redox potential of +0.353 V observed for complex **1** indicates that the ruthenium center is easily oxidizable. This is not surprising, because the electrolytically generated Ru(III) species could be easily stabilized by the hard phenoxide anion present in the complex. Complex **2** shows only one DPV peak at +0.505 V. It is possible that in this complex both the ruthenium center and the ferrocenyl moiety are getting oxidized at almost the same potential. In this complex the two electron-withdrawing chlorine atoms present in the ligand shift the redox potential to a more positive value. In order to understand these complicated Ru(II)/Ru(III) and Fe(II)/Fe(III) redox couples for these complexes better, complex **3**, which has the same ligand environment without the ferrocene moiety, has been prepared. The DPV of this complex shows only one peak at +0.374 V. This confirms that the redox peak observed at +0.353 V for the complex **1** corresponds to the Ru(II)/Ru(III) couple. If we look at the CV for the three complexes, complex **3** shows a clear one-electron Ru(II)/Ru(III) wave with a peak separation of 85 mV, whereas the other two complexes show a current intensity about 3 times that of complex **3** and have broad peaks with shoulders. The current intensity ratio of complexes **1** and **2** vs complex **3** is

dx.doi.org/10.1021/om3007882 | *Organometallics* 2012, 31, 6980–6987

Table 1. Absorption, Fluorescence, and Electrochemical Data of Synthesized Complexes 1−3 in Acetonitrile

complex	UV−visible λ_{max} (nm) (ε (M^{-1} cm^{-1}))	λ_{em} (λ_{ex}) (nm)	$E_{1/2}$(Ru(II)/Ru(III)), $E_{1/2}$(Fe(II)/Fe(III)) (V vs SCE)	ΔE (mV)
$[Ru(bpy)_2(L1)]PF_6$ (**1**)	~523.5 (7 400), ~466 (9 300), 345.5 (21 000), 294.5 (58 600), 243.0 (50 400)		+0.353, +0.485	140
$[Ru(bpy)_2(L2)]PF_6$ (**2**)	~510.5 (6 800) ~460.5 (8 050) 347.0 (19 000) 293.5 (47 150) 239.0 (43 100)		+0.505	217
$[Ru(bpy)_2(L3)]PF_6$ (**3**)	~525 (5 850) 344.5 (24 600) 292.0 (59 000) 246.0 (42 200)	562 (500)	+0.374	85

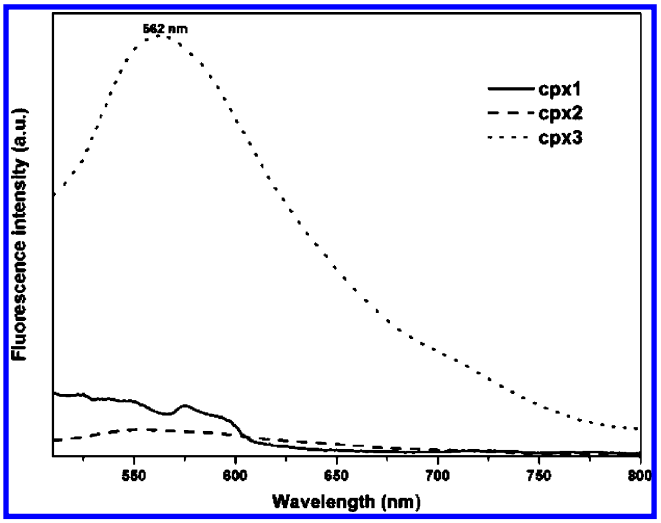

Figure 3. Fluorescence spectra of 20 μM solutions of complexes **1**−**3** in acetonitrile at 25 °C (excitation wavelength 500 nm).

about 3, indicating that a redox process takes place in all three metal centers in complexes **1** and **2**. The redox potentials of the ferrocene moieties are shifted to more positive potential in comparison to its free ligand form. Complex **2** has been structurally characterized by single-crystal X-ray diffraction technique. A single crystal of this compound was obtained by diffusion of diethyl ether vapor into an acetonitrile solution of the complex at room temperature. The crystallographic data for complex **2** are given in Table S2 (Supporting Information). An ORTEP view of complex **2** is shown in Figure 5. It can be seen from Figure 5 that the imidazole −NH group of the complex

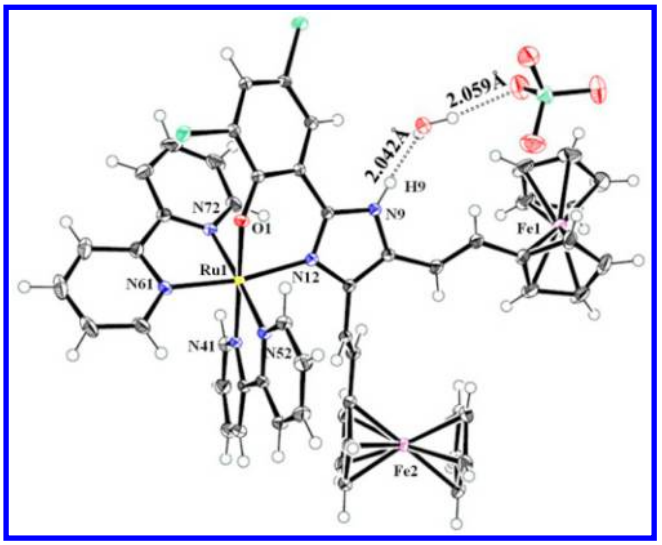

Figure 5. ORTEP diagram of complex **2**.

cation and the perchlorate anion (counterion) are connected by a hydrogen bond through the water of solvation. The phenol moiety and the imidazole are no longer coplanar in this case, unlike in the case of ligand **L2**, where they are coplanar.[11]

In complex **2** both the imidazole nitrogen and the phenolic oxygen are coordinated to the ruthenium(II) ion, and due to

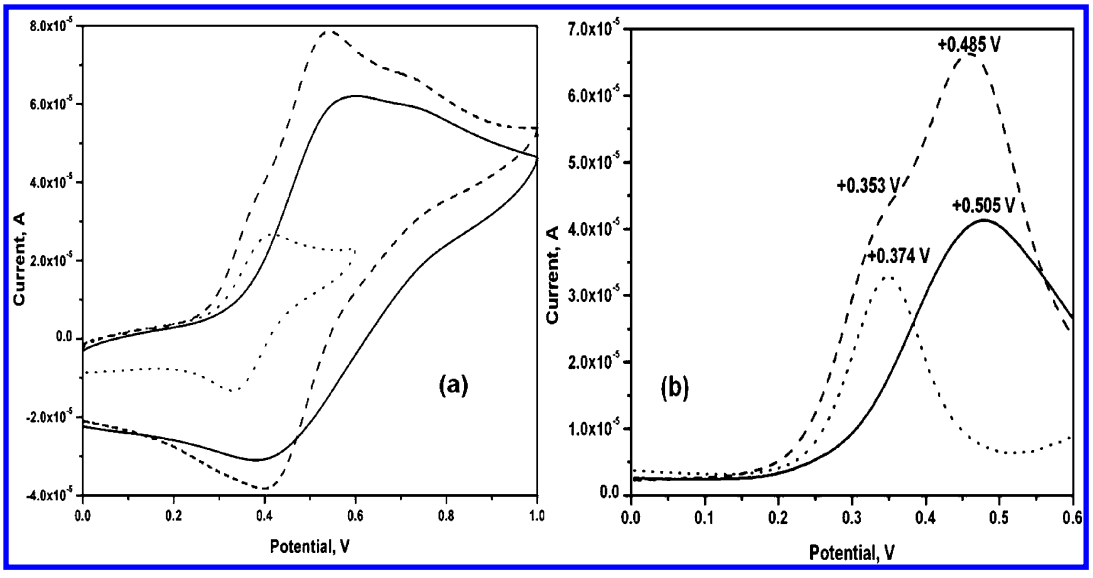

Figure 4. (a) Cyclic and (b) differential pulse voltammetry of complexes **1** (dashed line), **2** (solid line), **3** (dotted line) in acetonitrile (2 mM). The recorded potentials are referenced against the SCE at 25 °C at a scan rate of 100 mV s^{-1}.

dx.doi.org/10.1021/om3007882 | *Organometallics* 2012, 31, 6980−6987

the constraints of the octahedral geometry around the ruthenium(II) ion the phenol moiety and the imidazole moiety are not coplanar in this case; the dihedral angle between the phenol and imidazole moieties are 25°02′. The bite angles generated by the phenolate moiety and the imidazole moiety are less than 90°, as can be seen from Figure 6.

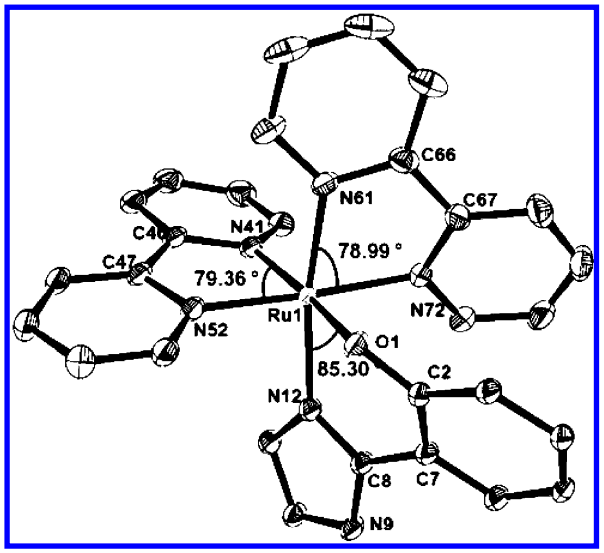

Figure 6. Pseudo-octahedral geometry around the central metal atom.

The two pyridine rings in the bipyridyl molecule are also not coplanar; the dihedral angles between the two rings are 4.8 and 10°. The ferrocene moieties are in different environments, and as a result the torsion angle between the Cp rings of ferrocene, the Fe−C and C−C bond lengths, and distance between Cp rings are not the same as in the case of the ligand. Interestingly, one of the ferrocene moieties shows a maximum torsion angle of 16°34′, which is halfway between staggered and eclipsed conformations (Table 2). The important bond lengths and

Table 2. Various Parameters Obtained from Crystal Structures of Ligands (L1 and L2) and Complex 2

compd		torsion angle	Fe−C bond length (Å)	C−C bond length (Å)	Cp distance (Å)
ferrocene[27]		36°	2.05	1.4	3.32
L1[a]	OH side	3°38′	2.043	1.429	3.285
	NH side	2°01′	2.049	1.426	3.302
L2[a]	OH side	6°21′	2.046	1.425	3.316
	NH side	5°17′	2.047	1.423	3.302
2	OH side	16°30′	2.042	1.424(5)	3.307
	NH side	4°43′	2.045	1.424(4)	3.296

[a]Reference 11.

bond angles for complex **2** are given in Table 3. Complex **2** has a one-dimensional hydrogen-bonding network between the imidazole −NH group, the water of solvation, and perchlorate anion, as shown in Figure S3 (Supporting Information). One can also see π stacking of bipyridyl moieties from two one-

Table 3. Important Bond Lengths (Å) and Bond Angles (deg) of Complex 2

Ru1−N61	2.0329(14)	Ru1−N72	2.0547(15)
Ru1−N41	2.0348(14)	Ru1−O1	2.0909(13)
Ru1−N52	2.0415(15)	Ru1−N12	2.0930(14)
N61−Ru1−N41	89.03(6)	N52−Ru1−O1	93.02(6)
N61−Ru1−N52	96.75(6)	N72−Ru1−O1	85.75(6)
N41−Ru1−N52	79.36(6)	N41−Ru1−N72	101.57(6)
N61−Ru1−N72	78.99(6)	N41−Ru1−N12	98.39(5)
N52−Ru1−N72	175.59(5)	N52−Ru1−N12	91.16(6)
N61−Ru1−O1	88.25(5)	N72−Ru1−N12	92.95(6)
N41−Ru1−O1	171.56(5)	O1−Ru1−N12	85.30(5)

dimensional networks in the crystal structure of the complex (Figure S3).

Interaction of Substituted Imidazole Phenol Mixed-Ligand Ruthenium(II) Complexes with DNA. *Absorption Spectral Titration.* Electronic absorption spectroscopy is one of the most useful techniques in DNA-binding studies. Since complexes **1**−**3** are coordinatively saturated and have no replaceable labile monodentate ligand in their coordination sphere, they are not expected to bind to DNA bases. These three complexes can either bind to DNA groove or bind to DNA intercalatively. Groove binding generally does not lead to well-defined changes in the energy of the absorption band, and in this case the intensity of the absorption band also does not show any marked change. Intercalative binding, on the other hand, generally gives rise to hypochromism with a red shift in the absorption bands of the molecule. No detectable changes in the energy of spectral bands of these complexes have been observed in the presence of DNA, ruling out an intercalative mode of binding of these three complexes.[12] The changes observed in the electronic spectrum of these three complexes in the presence of DNA can be rationalized in terms of groove binding.[13] However, since all three complexes contain aromatic rings in their ligand structure, partial intercalation of these molecules cannot be fully ruled out. The absorption spectra of the complexes **1**−**3** in the presence of increasing amounts of DNA are shown in Figure 7 and in Figures S4 and S5 (Supporting Information), respectively.

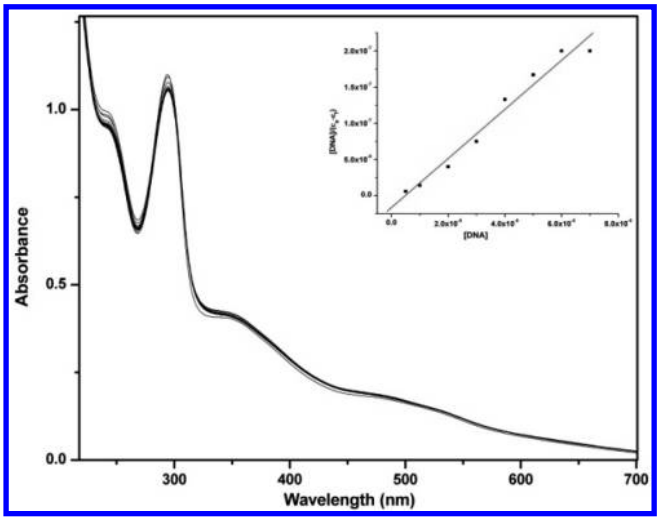

Figure 7. Absorption spectral titration of complex **1** (20 μM) with DNA (0−175 μM) in Tris buffer, pH 7.2.

dx.doi.org/10.1021/om3007882 | *Organometallics* 2012, 31, 6980−6987

None of the electronic spectra of three complexes show any clear isosbestic points during the successive addition of DNA. The intrinsic DNA binding constants, K_b, of the three complexes have been obtained by monitoring the changes in absorbance at 290 nm for complexes **1**−**3** with increasing concentrations of DNA. The DNA binding constants for complexes **1**−**3** have been found to be $(2.05 \pm 0.02) \times 10^5$, $(1.52 \pm 0.03) \times 10^5$, and $(1.43 \pm 0.03) \times 10^5$ M^{-1}, respectively.

Viscosity Measurements. Hydrodynamic methods are suitable for detection of small changes in the absence of crystallographic structural data and provide essential evidence to support an intercalation model. Intercalation of a molecule generally leads to an increase in the viscosity of DNA. In contrast, the molecules that bind to DNA either in the grooves or on the external surface give rise to irregularity or no changes in the viscosity of CT DNA. Figure 8 shows the changes in the viscosity of DNA on incremental addition of the ruthenium complexes **1**−**3**.

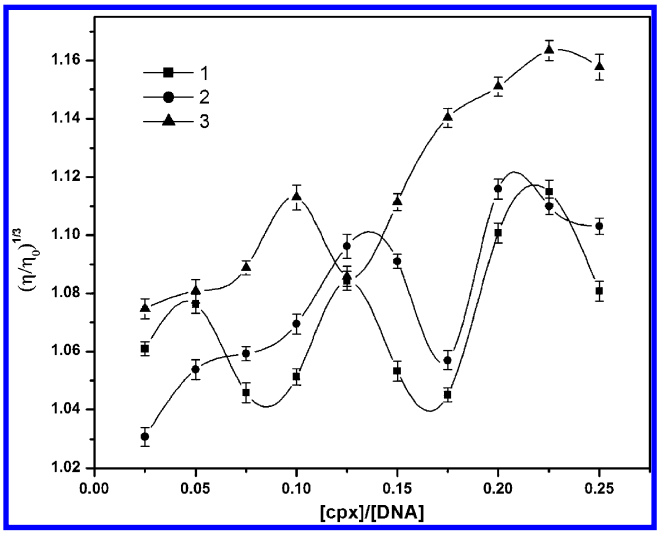

Figure 8. Relative viscosities of DNA solution in the presence of varying amounts of complexes **1**−**3**.

It is clear from the figure that the three complexes bring about irregular changes in the viscosity of DNA. This clearly rules out an intercalative mode of binding of these complexes to DNA. Though the complexes contain bipyridyl ligands, in the present case, it appears that the ancillary ligand, substituted imidazole phenol, dictates the mode of binding. Metal complexes containing bipyridyl ligands also have been shown to bind DNA non-intercalatively.[14] The presence of an −NH group in the imidazole would tend to favor hydrogen bonding with the base pairs of DNA rather than intercalation between the base pairs, thereby leading to groove binding of these complexes. A similar observation has been made in the case of imidazole-containing ferrocenyl compounds such as 2-ferrocenyl imidazophenanthroline and 2-ferrocenyl imidazophenanthrene.[15] Therefore, the results from the viscosity measurements confirm the groove binding of these complexes with DNA.

DNA Cleavage Activity. The DNA photocleavage activity of complexes **1**−**3** was studied by irradiating SC pUC19 DNA at 440 nm for 30 min in the presence of the three complexes (24 and 40 μM).

The results of these experiments are depicted in Figure 9. Out of the three complexes, complex **3**, which lacks a ferrocene

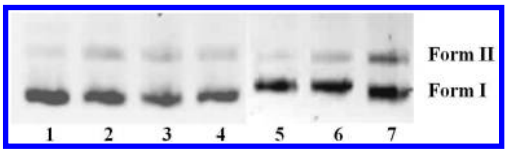

Figure 9. Cleavage of supercoiled pUC19 by complexes **1**−**3**, on incubation for 1 h followed by irradiation at 440 nm for 30 min: (lane 1) control DNA; (lanes 2−4) DNA in the presence of 24 μM complexes **1**−**3**, respectively; (lanes 5−7) pUC 19 DNA in the presence of 40 μM complexes **1**−**3**, respectively.

moiety, showed some photocleavage of plasmid SC DNA to NC DNA in the presence of 40 μM of the complex. At 60 μM concentration, complex **3** brought about 50% conversion of SC DNA to NC DNA (Figure 10). Conversion of SC DNA to NC

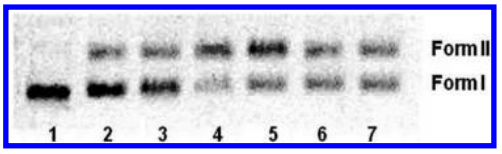

Figure 10. Cleavage of supercoiled pUC19 by complex **3**, on incubation for 1 h followed by irradiation at 440 nm for 30 min: (lane 1) control DNA; (lanes 2−6) pUC 19 DNA in the presence of 12, 24, 36, 48, and 60 μM of complex **3**, respectively; (lane 7) DNA in the presence of 60 μM complex **3** and 300 μM histidine.

DNA was observed even in the presence of histidine (singlet oxygen quencher), as can be seen from lane 7 of Figure 10. Hence, it is clear that cleavage of DNA in the presence of complex **3** under photolytic conditions is due to guanine oxidation by the excited state of ruthenium. It is of interest to note that complexes **1** and **2**, which have ferrocenyl moieties conjugated to the Ru(II) complex, did not show any significant photonuclease activity.

The oxidative cleavage of SC pUC19 DNA by complexes **1**−**3** was studied using hydrogen peroxide as an oxidizing agent. All three compounds showed cleavage in the presence of hydrogen peroxide (Figure 11).

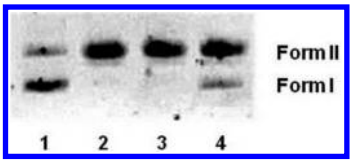

Figure 11. Oxidative cleavage of supercoiled pUC19 in the absence (lane 1) and presence of complexes **1**−**3** (24 μM; lanes 2−4, respectively) and 240 μM H_2O_2 on incubation for 1 h.

Iron(II) is known for its Fenton chemistry with hydrogen peroxide and is known to form $^{\bullet}OH$ and $^{\bullet}OOH$ radicals. In this case complexes **1** and **2** have Fe(II) and Ru(II) metal ions and complex **3** has only the Ru(II) metal ion. The redox potentials of these metal ions are low enough in complexes **1**−**3**, and hence, the metal ions can be oxidized to their higher valences as in the case of the Fenton reaction. The redox potential of the metal complex is an important parameter for the generation of hydroxyl and peroxide radicals under the experimental conditions for the nicking of DNA.[16]

dx.doi.org/10.1021/om3007882 | *Organometallics* 2012, 31, 6980−6987

The DNA cleavage efficiency of these complexes in the presence of hydrogen peroxide shows that 24 μM of complexes **1** and **2** is able to cleave DNA completely, whereas 24 μM of complex **3** is not able to convert form I to form II completely. This may be due to the fact that complexes **1** and **2** have three potential active metal ions that can generate 3 times more radical species in comparison to complex **3**, which has only one such metal ion in a molecule.

CONCLUSIONS

Ferrocene conjugated ruthenium complexes have attracted the attention of researchers because of their application in chemotherapy. Conjugation of the ferrocene molecule to ruthenium(II) complexes is expected to lead to changes in the photophysical properties of the ruthenium(II) center as well as the DNA-cleaving properties of the ruthenium(II) complex. Three ruthenium(II) complexes with general formula $[Ru(bpy)_2L](PF_6)$ (**1**−**3**), where L = 2-{4,5-bis[(*E*)-2-ferrocenylvinyl]-1*H*-imidazol-2-yl}phenol (**1**), 2-{4,5-bis[(*E*)-2-ferrocenylvinyl]-1*H*-imidazol-2-yl)-4,6-dichlorophenol (**2**), 2-{4,5-bis[(*E*)-2-(4-chlorophenyl)ethenyl]-1*H*-imidazol-2-yl}-phenol (**3**), have been synthesized and characterized spectroscopically and electrochemically. Complexes **1** and **2** contain two conjugated ferrocene molecules, whereas complex **3** lacks a conjugated ferrocene molecule. Complex **2** has also been crystallographically characterized. Electronic spectra of all three complexes show the MLCT band of the ruthenium(II) center at 540 nm. Complexes **1** and **2** also exhibit ligand field transitions associated with the ferrocenyl moiety. Complex **3** upon excitation at its MLCT band shows emission from the MLCT excited state of the ruthenium(II) center. On the other hand, complexes **1** and **2** do not exhibit emission from the MLCT excited states of their respective ruthenium(II) centers, due to quenching of their excited states by the ferrocenyl moiety present in these two complexes. The DPV of complex **1** shows redox peaks at +0.353 V due to the Ru(II)/Ru(III) couple and at +0.485 V due to the Fe(II)/Fe(III) redox couple. Complex **3**, which does not contain a conjugated ferrocene moiety, shows only one DPV peak at +0.353 V. This conclusively proves that the redox peak observed in the DPV of complex **1** at +0.353 V is due to the Ru(II)/Ru(III) couple. The Ru(II)/Ru(III) redox potential of +0.353 V observed for complex **1** indicates that the ruthenium center is easily oxidizable. This is not surprising, because the electrolytically generated Ru(III) species could be easily stabilized by the hard phenoxide anion present in the complex. Complex **2** shows only one DPV peak at +0.505 V. It is possible that in this complex both the ruthenium center and the ferrocenyl moiety are oxidized at almost the same potential. In this complex the two electron-withdrawing chlorine atoms present in the ligand shift the redox potential to more positive values. The values of diffusion currents in the case of complexes **1** and **2** have been found to be almost 3 times that observed for complex **3**. This is because of the fact that in complexes **1** and **2** the redox process takes place at three metal centers, whereas in complex **3** there is only one redox-active metal center. All three complexes have been found to exhibit groove binding to CT DNA. Complex **3**, which contains only Ru(II) as the redox-active metal ion, exhibits photonuclease activity, whereas complexes **1** and **2**, which have conjugated ferrocenyl moieties, do not show any photonuclease activity. All three complexes exhibit nuclease activity in the presence of H_2O_2. Complexes **1** and **2** exhibit enhanced nuclease activity in comparison to complex **3** due to the presence of three redox-active metal centers in complexes **1** and **2**. Complex **3**, which has only one redox-active metal center, evidently shows lower nuclease activity. Studies on the antiproliferative activity of these three complexes on cancer cell lines are currently in progress, and the results will be reported subsequently.

EXPERIMENTAL SECTION

Materials and Methods. Ruthenium chloride trihydrate, ferrocenecarboxaldehyde, biacetyl, piperidine, salicylaldehyde, 3,5-dichlorosalicylaldehyde, and 4-chlorobenzaldehyde were purchased from Aldrich. Plasmid DNA pUC-19, suitable for gel electrophoresis, was purchased from Genie, Bangalore, India, and used as received. Calf thymus DNA (CT DNA) and agarose were procured from SRL (India). Acetonitrile, dimethyl sulfoxide, dichloromethane, ethanol, and methanol were of chromatographic grade and were used without further purification. Tris(hydroxymethyl)aminomethane-HCl (Tris-HCl) buffer was prepared using deionized and degassed triple-distilled water. All the experiments regarding the binding and cleavage of DNA using complexes **1**−**3** were carried out in Tris buffer (pH, 7.2). A solution of CT DNA in the buffer gave a ratio of UV absorbance at 260 and 280 nm of about 1.8−1.9, indicating that the DNA was sufficiently free from protein.[17] The DNA concentration per nucleotide was determined by absorption spectroscopy using molar absorption coefficient as 6600 M^{-1} cm^{-1} at 260 nm.[18]

Physical Measurements. Absorption spectra were recorded on a Shimadzu UV-160A UV−visible recording spectrophotometer; emission spectra were recorded on a Varian Cary Eclipse spectrofluorometer. ESI mass spectra were obtained from a Finnigan LCQ Advantage max ion trap mass spectrometer. Elemental analysis was carried out using a Euro Vector C,H,N analyzer. Viscosity experiments were made with an Ostwald viscometer, immersed in a water bath maintained at 25 °C. All cyclic (CV) and differential pulse (DPV) voltammetry experiments were conducted on a CH Instruments (USA) Model CH-620 B electrochemical analyzer. Tetrabutylammonium perchlorate (TBAP) was used as the supporting electrolyte. The sample, dissolved in dried acetonitrile, was purged with nitrogen prior to each electrochemical measurement. A standard three-electrode system comprised of glassy carbon as the working electrode, platinum electrode as the auxiliary electrode, and saturated calomel as the reference electrode (SCE) was used.

Synthesis of 2-(4,5-Bis((*E*)-2-ferrocenylvinyl)-1*H*-imidazol-2-yl)phenol (L1) and 2-(4,5-Bis((*E*)-2-ferrocenylvinyl)-1*H*-imidazol-2-yl)-4,6-dichlorophenol (L2). 2-(4,5-Bis((*E*)-2-ferrocenylvinyl)-1*H*-imidazol-2-yl)phenol and 2-(4,5-bis((*E*)-2-ferrocenylvinyl)-1*H*-imidazol-2-yl)-4,6-dichlorophenol were prepared according to the procedure available in the literature.[11]

Synthesis of 2-{4,5-Bis[(*E*)-2-(4-chlorophenyl)ethenyl]-1*H*-imidazol-2-yl}phenol (L3). 1,6-Bis(chlorophenyl)hexa-1,5-diene-3,4-dione[19] (0.5 g, 1.51 mmol), salicylaldehyde (0.185 g, 1.51 mmol), and ammonium acetate (2 g, 25 mmol) were dissolved in 15 mL of acetic acid and heated to reflux for 3 h.[20] After cooling, cold water (10 mL) was added to the solution, during which a yellow precipitate appeared. The precipitate was filtered, washed using cold water, and purified by column chromatography on silica gel with ethyl acetate/hexane (1/4) as eluent to give the product. Yield: 0.35 g, 54%. ESI-MS: 434 $(M + 1)^+$. Anal. Calcd for $C_{25}H_{18}Cl_2N_2O$: C, 69.29; H, 4.19; N, 6.46. Found: C, 69.20; H, 4.25; N, 6.59.

Synthesis of $[Ru(bpy)_2(L1)](PF_6)$ (1). A mixture of [*cis*-$Ru(bpy)_2Cl_2]\cdot 2H_2O$[21] (0.18 g, 0.34 mmol) and **L1** (0.2 g, 0.34 mmol) in the presence of Et_3N (50 μL) was suspended in an EtOH/H_2O solvent mixture (3/1, v/v). The mixture was refluxed under an inert atmosphere for 4 h while vigorous stirring was maintained. The reaction mixture was cooled to room temperature; the solvent was reduced under vacuum to one-third of its initial volume. A saturated aqueous solution of NH_4PF_6 was added to precipitate $[Ru(bpy)_2(\mathbf{L1})]^+$ as its hexafluorophosphate salt. The product was filtered and washed with water (3 × 10 mL) and then purified by column chromatography on neutral alumina using acetonitrile/toluene (1.5/1,

dx.doi.org/10.1021/om3007882 | *Organometallics* 2012, 31, 6980−6987

v/v) as eluent. Yield: 0.37 g, 95%, Anal. Calcd for $C_{53}H_{43}F_6Fe_2N_6OPRu$: C, 55.95; H, 3.81; N, 7.39. Found: C, 55.90; H, 3.88; N, 7.27. ESI-MS: m/z 993 $(M - PF_6)^+$. IR (cm^{-1}; KBr pellet): 3402, 3085, 1600, 1477, 1265, 844.

Synthesis of $[Ru(bpy)_2(L2)](PF_6)$ (2). The synthesis and purification of compound **2** were similar to those of **1** using $[Ru(bpy)_2Cl_2]\cdot 2H_2O$ (0.2 g, 0.38 mmol) and **L2** (0.25 g, 0.38 mmol). Yield: 0.43 g, 93%, Anal. Calcd for $C_{53}H_{41}Cl_2F_6Fe_2N_6OPRu$: C, 52.76; H, 3.42; N, 6.97. Found: C, 52.68; H, 3.49; N, 6.89; ESI-MS: m/z 1061.93 $(M - PF_6)^+$. IR (cm^{-1}; KBr pellet): 3082, 2927, 1600, 1461, 1122, 1107, 763. The perchlorate salt of complex **2** was prepared for single-crystal X-ray diffraction studies by addition of excess sodium perchlorate instead of ammonium hexafluorophosphate as the precipitating agent. Single crystals of this molecule have been obtained by diffusion of diethyl ether into a solution of the compound in an acetonitrile/water mixture (95/5).

Synthesis of $[Ru(bpy)_2(L3)](PF_6)$ (3). This compound was synthesized and purified by a procedure similar to that described for compound **1**, except that **L3** (0.5 g, 1.15 mmol) was used instead of **L1**. Yield: 1.09 g, 96%, Anal. Calcd for $C_{45}H_{33}Cl_2F_6N_6OPRu$: C, 54.55; H, 3.36; N, 8.48. Found: C, 54.48; H, 3.29; N, 8.41; ESI-MS: m/z 845.07 $(M - PF_6)^+$. IR (cm^{-1}; KBr pellet): 3398, 3066, 1600, 1485, 1091, 1014, 844.

X-ray Crystallographic Data Collection and Refinement of the Structure. A red single crystal of the compound $[Ru(bpy)_2(L2)](ClO_4)\cdot H_2O$ was coated with perfluoropolyether, picked up with a nylon loop, and immediately mounted in the nitrogen cold stream of a Bruker-Nonius KappaCCD diffractometer equipped with a Mo-target rotating-anode X-ray source. Graphite-monochromated Mo Kα radiation (λ = 0.710 73 Å) was used. Final cell constants were obtained from least-squares fits for all measured reflections. Intensity data were corrected for absorption using intensities of redundant reflections with the program SADABS.[22] The structure was readily solved by Patterson methods and subsequent difference Fourier techniques. The Siemens ShelXTL[23] software package was used for the solution and creation of artwork of the structures; ShelXL97[24] was used for the refinement. All the non-hydrogen atoms were anisotropically refined, and hydrogen atoms bound to carbon were placed at calculated positions and refined as riding atoms with isotropic displacement parameters. Hydrogen atoms bound to nitrogen and oxygen were located from the difference map. Crystallographic data of the compound are given in Table S2 (Supporting Information). CCDC reference number: 837444.

Absorption Titration. Calf thymus (CT) DNA solutions of various concentrations (5−175 μM) were added to the metal complex (20 μM dissolved in 10% CH_3CN/10 mM tris HCl, pH 7.2), and the MLCT transitions of complexes **1**−**3** were monitored. The absorption spectra were recorded after 10 min of incubation. The nature of equilibrium DNA binding constants, K_b, was calculated from the eq 1,

$$[DNA]/(\varepsilon_a - \varepsilon_f) = [DNA]/(\varepsilon_b - \varepsilon_f) + 1/K_b(\varepsilon_b - \varepsilon_f) \quad (1)$$

where ε_a, ε_f, and ε_b correspond to $A_{obsd}/[Ru]$, the extinction coefficient for the free ruthenium complex, and the extinction coefficient for the ruthenium complexes in the fully bound form, respectively. A plot of $[DNA]/(\varepsilon_a - \varepsilon_f)$ versus $[DNA]$ gives K_b as the ratio of the slope to the intercept.[25]

Viscosity Studies. Viscosity experiments were performed using an Ostwald viscometer of 3 mL capacity. A viscometer was thermostated in a water bath to maintain constant temperature (28 °C). The concentration of DNA (200 μM) was kept constant, and the concentrations of metal complexes were varied (0−50 μM). The flow times for the buffer (10 mM Tris-HCl), DNA alone, and DNA in the presence of ruthenium complexes were monitored at least three times using a manually operated digital stopwatch, and an average flow time was calculated. The relative specific viscosity was calculated using the equation $\eta = (t - t_0)/t_0$, where t_0 is the flow time for the buffer and t is the observed flow time for DNA in the absence and presence of complex. A plot of $(\eta/\eta_0)^{\wedge}(1/3)$ vs $(1/R)$ (R = [DNA]/[complex]), where η is the viscosity of DNA in the presence of the complex and η_0 is the viscosity of DNA alone, was constructed from viscosity measurements.[26]

DNA Cleavage Studies. Photonuclease activity of the complexes was monitored using gel electrophoresis of plasmid DNA (pUC19). Two sets of 25 μL solutions were prepared for the photolysis experiment. One set of solutions contained 3 μL of 100 μg/mL of plasmid DNA in Tris buffer with varying amounts of metal complex **1**−**3** (0−24 μM). Each solution was incubated for 1 h and then irradiated at 440 nm for various time intervals varying from 10 to 60 min. The samples were then subjected to electrophoresis in 0.8% agarose gel (tris-boric acid-EDTA buffer, pH 8.0) at 50 V for 2 h. The gel was stained with 0.5 μg/mL of ethidium bromide. The stained gel was illuminated under an UV lamp and gel documented. In a separate experiment the DNA was incubated with 24 μM of the metal complex and 240 μM of histidine and irradiated at 440 nm. The photolyzed solution was subsequently subjected to electrophoresis. Also, oxidative cleavage of DNA with complexes **1**−**3** in the presence of hydrogen peroxide as an oxidizing agent was studied. A 3 μL portion of 100 μg/mL of plasmid DNA in Tris buffer with metal complex **1**−**3** (24 μM) and 240 μM of H_2O_2 was prepared. Each solution was incubated for 1 h before being subjected to electrophoresis.

■ ASSOCIATED CONTENT

Ⓢ Supporting Information

Figures, a table, and a CIF file giving mass spectra of synthesized compounds, crystallographic data of complex **2**, and absorption spectral titration of complexes **2** and **3**. This material is available free of charge via the Internet at http://pubs.acs.org.

■ AUTHOR INFORMATION

Corresponding Author

*E-mail: bunair@clri.res.in.

Notes

The authors declare no competing financial interest.

■ ACKNOWLEDGMENTS

We thank the Council of Scientific and Industrial Research, New Delhi (for a research fellowship to G.S.).

■ REFERENCES

(1) Reddy, H. *Bioinorganic Chemistry*; New Age International: New Delhi, 2005.

(2) Köpf, H.; Köpf-Maier, P. *Angew. Chem.* **1979**, *91*, 509−512.

(3) (a) Edwards, E. I.; Epton, R.; Marr, G. *J. Organomet. Chem.* **1976**, *122*, C49−C53. (b) Edwards, E. I.; Epton, R.; Marr, G.; Rogers, G. K.; Thompson, K. *J. Spec. Publ. Chem. Soc.* **1977**, *128*, 92−100. (c) Simionescu, C.; Lixandru, T.; Tataru, L.; Mazilu, I.; Vata, M.; Luca, S. *J. Organomet. Chem.* **1983**, *252*, C43−C46. (d) Scutaru, D.; Tataru, L.; Mazilu, I.; Diaconu, E.; Lixandru, T.; Simionescu, C. *J. Organomet. Chem.* **1991**, *401*, 81−85. (e) Scutaru, D.; Mazilu, I.; Vata, M.; Tataru, L.; Vlase, A.; Lixandru, T.; Simionescu, C. *J. Organomet. Chem.* **1991**, *401*, 87−90.

(4) (a) Sawamura, M.; Sasaki, H.; Nakata, T.; Ito, Y. *Bull. Chem. Soc. Jpn.* **1993**, *66*, 2725−2729. (b) Biot, C.; Delhaes, L.; Maciejewski, L. A.; Mortuaire, M.; Camus, D.; Dive, D.; Brocard, J. S. *Eur. J. Med. Chem.* **2000**, *35*, 707−714. (c) Beagley, P.; Blackie, M. A. L.; Chibale, K.; Clarkson, C.; Meijboom, R.; Moss, J. R.; Smith, P. J.; Su, H. *Dalton Trans.* **2003**, 3046−3051. (d) Top, S.; Vessieres, A.; Leclercq, G.; Quivy, J.; Tang, J.; Vaissermann, J.; Huche, M.; Jaouen, G. *Chem. Eur. J.* **2003**, *9*, 5223−5236.

(5) (a) Ang, W. H.; Daldini, E.; Scolaro, C.; Scopelliti, R.; Juillerat-Jeannerat, L.; Dyson, P. J. *Inorg. Chem.* **2006**, *45*, 9006−9013. (b) Süss-Fink, G. *Dalton Trans.* **2010**, *39*, 1673−1688. (c) Mishra, A.;

Jung, H.; Park, J. W.; Kim, H. K.; Kim, H.; Stang, P. J.; Chi., K.-W. *Organometallics* **2012**, *31*, 3519−3526.
(6) (a) Erkkila, K. E.; Odom, D. T.; Barton, J. K. *Chem. Rev.* **1999**, *99*, 2777−2795. (b) Metcalfe, C.; Thomas, J. A. *Chem. Soc. Rev.* **2003**, *32*, 215−224. (c) Sigman, D. S.; Mazumder, A.; Perrin, M. D. *Chem. Rev.* **1993**, *93*, 2295−2316. (d) Dandlier, P. J.; Holmlin, R. E.; Barton, J. K. *Science* **1997**, *274*, 1465−1468. (e) Elias, B.; Kirsh De Mesmaeker, A. *Coord. Chem. Rev.* **2006**, *250*, 1627−1641. (f) Turro, N. J.; Barton, J. K.; Tomalia, D. A. *Acc. Chem. Res.* **1991**, *24*, 332−340.
(7) Maurya, M. R.; Woo, L. K. *J. Organomet. Chem.* **2005**, *690*, 4978−4981.
(8) (a) Liu, H. -K.; Berners-Price, S. J.; Wang, F.; Parkinson, J. A.; Xu, J.; Bella, J.; Sadler, P. J. *Angew. Chem., Int. Ed.* **2006**, *45*, 8153−8156. (b) Bergamo, A.; Sava, G. *Dalton Trans.* **2007**, 1267−1272.
(9) (a) Lednicer, D.; Mitscher, L. L. *The Organic Chemistry of Drug Synthesis*; Wiley-Interscience: New York, 2005; Vol. 2, pp 242−260. (b) Laurence, B. L.; John, S. L.; Keith, P. L *Goodman and Gilman's the Pharmacological Basis of Therapeutics*; McGraw-Hill: New York, 2000; pp 986−1032.
(10) Fery-Forgues, S.; Delavaux-Nicot, B. *J. Photochem. Photobiol. A: Chem.* **2000**, *132*, 137−159.
(11) Sathyaraj, G.; Muthamilselvan, D.; Kiruthika, M.; Weyhermüller, T.; Nair, B. U. *J. Organomet. Chem.* **2012**, *716*, 150−158.
(12) (a) Barton, J. K.; Dannenberg, J. J.; Raphael, A. L. *J. Am. Chem., Soc.* **1984**, *106*, 2172−2176. (b) Tysoe, S. A.; Morgan, R. J.; Baker, A. D.; Strekas, T. C. *J. Phys. Chem.* **1993**, *97*, 1707−1711.
(13) Vijayalakshmi, R.; Kanthimathi, M.; Subramanian, V.; Nair, B. U. *Biochem. Biophys. Acta* **2000**, *1475*, 157−164.
(14) Kumar, C. V.; Barton, J. K.; Turro, J. J. *J. Am. Chem. Soc.* **1985**, *107*, 5518−5523.
(15) (a) Zhao, X. -L.; Han, M. -J.; Zhang, A. -G.; Wang, K. -Z. *J. Inorg. Biochem.* **2012**, *107*, 104−110. (b) Maity, B.; Chakravarthi, B. V. S. K.; Roy, M.; Karande, A. A.; Chakravarty, A. R. *Eur. J. Inorg. Chem.* **2011**, 1379−1386.
(16) Indumathy, R.; Kanthimathi, M.; Weyhermüller, T.; Nair, B. U. *Polyhedron* **2008**, *27*, 3443−3450.
(17) Marmur, J. *J. Mol. Biol.* **1961**, *3*, 208−218.
(18) Reichmann, R. E.; Rice, S. A.; Thomas, C. A.; Doty, P. J. *J. Am. Chem. Soc.* **1954**, *76*, 3047−3053.
(19) Króhnke, F. *Synthesis* **1976**, *1*, 1−24.
(20) Davidson, D.; Weiss, M.; Jelling, M. *J. Org. Chem.* **1937**, *2*, 319−327.
(21) Sullivan, B. P.; Salmon, D. J.; Meyer, T. *J. Inorg. Chem* **1978**, *17*, 3334−3341.
(22) Sheldrick, G. M. *SADABS, Bruker−Siemens Area Detector Absorption and Other Correction, Version 2006/1*; University of Göttingen, Göttingen, Germany, 2006.
(23) *ShelXTL 6.14*; Bruker AXS Inc., Madison, WI, 2003.
(24) Sheldrick, G. M. *ShelXL97*; University of Göttingen, Göttingen, Germany, 1997.
(25) Wolfe, A.; Shimer, G. H.; Meehan, T. *Biochemistry* **1987**, *26*, 6392−6396.
(26) Cohen, G.; Eisenberg, H. *Biopolymers* **1969**, *8*, 45−55.
(27) Dunitz, J. D.; Orgel, L. E.; Rich, A. *Acta Crystallogr.* **1956**, *9*, 373−375.